

# INTRINSIC DIMENSION ESTIMATION VIA NEAREST CONSTRAINED SUBSPACE CLASSIFIER

LIANG LIAO, YANNING ZHANG, STEPHEN JOHN MAYBANK, ZHOUFENG LIU

LIAOLIANGIS@126.COM (L. LIAO), SJMAYBANK@DCS.BBK.AC.UK (S. J. MAYBANK)

**ABSTRACT.** We consider the problems of classification and intrinsic dimension estimation on image data. A new subspace based classifier is proposed for supervised classification or intrinsic dimension estimation. The distribution of the data in each class is modeled by a union of a finite number of affine subspaces of the feature space. The affine subspaces have a common dimension, which is assumed to be much less than the dimension of the feature space. The subspaces are found using regression based on the  $\ell_0$ -norm. The proposed method is a generalisation of classical NN (Nearest Neighbor), NFL (Nearest Feature Line) classifiers and has a close relationship to NS (Nearest Subspace) classifier. The proposed classifier with an accurately estimated dimension parameter generally outperforms its competitors in terms of classification accuracy. We also propose a fast version of the classifier using a neighborhood representation to reduce its computational complexity. Experiments on publicly available datasets corroborate these claims.

**KEYWORDS.** Intrinsic dimension estimation, Nearest constrained subspace classifier, Image classification, Sparse representation

## 1. INTRODUCTION

The concept of data manifold plays a vital role in pattern recognition. Briefly speaking, a data manifold is a topological space which contains the data samples, and which serves as an ideal geometric description of the data. In this description, all data points, including the observed and unobserved, lie in a data manifold, whose dimension is often much lower than the dimension of the feature space which contains it.

In previous work, the manifold model has been used as a powerful analytical approximation tool for nonparametric signal classes such as human face images or handwritten digits [1, 2, 3]. If the data manifold is learned, then it can be exploited for classifier design. The manifold learning usually involves constructing a mapping from the feature space to a lower-dimensional space that is adapted to the training data and that preserves the proximity of data points to each other.

There have been many works on manifold learning. For example, methods such as ISOMAP (ISometric Mapping) [4], Hessian Eigenmaps (also known as HLLLE, Hessian Locally Linear Embedding) [5], LLE (Local Linear Embedding) [6], Maximum Variance

Unfolding (MVU) [7], Local Tangent Space Alignment (LTSA) [8] and Laplacian Eigenmap [9] have been introduced. These methods learn a low-dimensional manifold under the constraint that the proximity properties of the nearby data are preserved.

We propose a novel supervised classifier framework in which each class is modeled by a union of a finite number of affine subspaces. The proposed algorithm is superior to the traditional classifiers such as NN (Nearest Neighbor), NFL (Nearest Feature Line, proposed by S. Z. Li [10]), NS (Nearest Subspace), etc., because the use of finite affine subspaces allows a more accurate description of the distribution of the data.

The remainder of this paper is organized as follows. In Section 2, some background and related works about the classical classifiers including NN (Nearest Neighbor), NFL (Nearest Feature Line) and NS (Nearest Subspace) are briefly revisited. In Section 3, the classification model of NM (Nearest Manifold) and some classifier design principles are presented. Then, a novel constrained subspace framework named NCSC and its fast version are proposed in Section 4. Section 5 gives the experimental results on several publicly available datasets. In Section 6, some concluding remarks are given.

## 2. BACKGROUND AND RELATED WORKS

We argue that the NN, NFL and NS classifiers can be incorporated into a unified framework. Before the detailed discussion, let's first briefly revisit the theoretical background.

**2.1. NN and NFL.** The NN, NFL and NS classifiers base the classification of a sample  $\mathbf{y}$  on the distances measured in the feature space.

For NN and NFL, there exists a convenient geometrical interpretation — given  $N_i$  training samples in a given class (say, the  $i$ -th class), the distances are obtained as illustrated in Figure 1 where to simplify the explanations, we set  $N_i = 3$ .

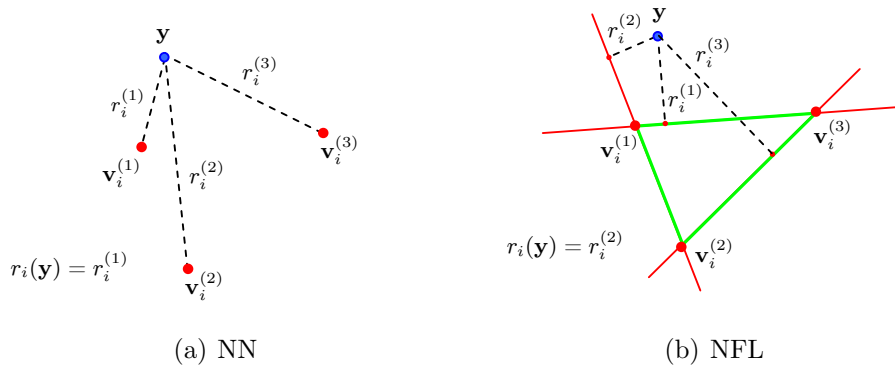


FIGURE 1. The distances of a query sample  $\mathbf{y}$  in NN and NFL to a class (the  $i$ -th, as shown), where  $N_i = 3$ .

In Figure 1(a), the distance from  $\mathbf{y}$  to the  $i$ -th class is the minimum  $r_i(\mathbf{y})$  of the distances from  $\mathbf{y}$  to the training samples in the  $i$ -th class. In Figure 1(b), each pair of training samples defines a line. The distance from  $\mathbf{y}$  to the  $i$ -th class is defined as the minimum  $r_i(\mathbf{y})$  of the distances from  $\mathbf{y}$  to the different lines.

More generally, given the training samples  $\mathbf{v}_i^{(1)}, \dots, \mathbf{v}_i^{(N_i)}$  of the  $i$ -th class, in NN,  $r_i(\mathbf{y})$  is written as

$$r_i(\mathbf{y}) = \min_{j \in \{1, \dots, N_i\}} \left\| \mathbf{y} - \mathbf{v}_i^{(j)} \right\|_2. \quad (2.1)$$

In NFL,  $r_i(\mathbf{y})$  is defined as

$$r_i(\mathbf{y}) = \min_{\lambda \in \mathbb{R}, a, b \in \{1, \dots, N_i\}} \left\| \mathbf{y} - \lambda \mathbf{v}_i^{(a)} - (1 - \lambda) \mathbf{v}_i^{(b)} \right\|_2. \quad (2.2)$$

**2.2. NS.** In NS, the minimum distance  $r_i(\mathbf{y})$  is the projection distance from  $\mathbf{y}$  to the subspace linearly spanned by all the training samples in the  $i$ -th class.

More specifically, given  $N_i$  training samples in the  $i$ -th class, define

$$\mathbf{V}_i = \left[ \mathbf{v}_i^{(1)}, \dots, \mathbf{v}_i^{(N_i)} \right] \quad (2.3)$$

where  $\mathbf{v}_i^{(j)} \in \mathbb{R}^D$  is the  $j$ -th training sample and  $D$  is the feature dimension.

Note that we assume that the training samples  $\mathbf{v}_i^{(1)}, \dots, \mathbf{v}_i^{(N_i)}$  are linearly independent. Namely,  $\mathbf{V}_i \in \mathbb{R}^{D \times N_i}$  is a full rank matrix, satisfying  $D \geq N_i$ . Henceforth, unless otherwise stated, we assume that the given training samples are linearly independent. This assumption is satisfied in many pattern recognition problems in which the feature space has a high dimension.

Then, in NS,  $r_i(\mathbf{y})$  is defined as

$$r_i(\mathbf{y}) = \min_{\boldsymbol{\alpha}_i \in \mathbb{R}^{N_i}} \left\| \mathbf{y} - \mathbf{V}_i \boldsymbol{\alpha}_i \right\|_2 \quad (2.4)$$

where  $\boldsymbol{\alpha}_i \doteq \left[ \alpha_i^{(1)}, \dots, \alpha_i^{(N_i)} \right]^T$  is the coefficient vector.

If the  $N_i$  training samples are linearly independent, the spanned subspace is  $N_i$ -dimensional.

After the distances from  $\mathbf{y}$  to  $K$  classes are obtained, NN, NFL and NS, using the same scheme, determine the class of  $\mathbf{y}$  by

$$\text{class}(\mathbf{y}) = \arg \min_{i \in \{1, \dots, K\}} r_i(\mathbf{y}). \quad (2.5)$$

### 3. NM: NEAREST MANIFOLD

The NM (Nearest Manifold) classifier is a generalization of the NN, NFL and NS classifiers. It also determines the class of a query sample based on the minimum distance.

In NM, the manifold associated with a given class is a topological space such that all the data points (including the observed ones and unobserved ones) of the class are lying on or near to it. Thus, the manifold dimension is actually the intrinsic dimension of the dataset and is usually much less than the dimension of feature space. If a query data sample is near to a data manifold, then it is assigned to the corresponding class.

**3.1. Model.** For a given a class, we define its universal dataset to be the “conceptual” set containing all the observed and unobserved data of this class. It is assumed that this universal data set forms a manifold in the feature space, and that the dimension of the manifold is much less than the dimension of the feature space.

Given  $K$  data manifolds denoted by  $\mathcal{M}_1, \dots, \mathcal{M}_K$ ,  $\mathbf{y}$  is assigned to the class whose data manifold is the nearest to  $\mathbf{y}$ . More specifically,  $r_i(\mathbf{y})$  is written as follows.

$$r_i(\mathbf{y}) = \min_{\mathbf{z} \in \mathcal{M}_i} \|\mathbf{y} - \mathbf{z}\|_2, \quad \forall i = 1, \dots, K. \quad (3.1)$$

After that, NMC (Nearest Manifold Classifier) uses Equation (2.5) to classify  $\mathbf{y}$ .

**3.2. Classifier Design Based on the Least Distance.** Although it is difficult to implement the NM classifier primarily due to the difficulty of deducing the  $K$  data manifolds from the given training samples, the NM model gives us some clues for designing a good classifier based on the nearest distance.

Given the training sets for each of  $K$  classes, a good classifier can be obtained by adding new derived points to the training sets. In NFL, the derived points consist of points on the feature lines of the class. In NS, the derived points consist of the subspaces spanned by the training samples of the class. The solution of NM is to use data manifolds  $\mathcal{M}_1, \dots, \mathcal{M}_K$  to replace the training sets.

From this point of view, NFL, and NS are approximations to NM in that the training sets and the derived points approximate the data manifolds. But these approximations are not necessarily the best.

#### 4. NEAREST CONSTRAINED SUBSPACE CLASSIFIER

We propose a novel classifier called the nearest constrained subspace classifier (NCSC), which generalizes NN, NFL and has a close relationship to NS. The proposed classifier is formulated as the solution to a problem of constrained least-squares regression, i.e.  $\ell_2$ -norm minimization.

**4.1. Coefficient Constraints.** Given  $N_i$  training samples  $\mathbf{v}_i^{(1)}, \dots, \mathbf{v}_i^{(N_i)}$  in the  $i$ -th class ( $\forall i = 1, \dots, K$ ), NCSC defines  $r_i(\mathbf{y})$  as

$$\begin{aligned} r_i(\mathbf{y}) &= \min_{\boldsymbol{\alpha}_i \in \mathbb{R}^{N_i}} \|\mathbf{y} - \mathbf{V}_i \boldsymbol{\alpha}_i\|_2 \\ \text{subject to } &\sum_{j=1}^{N_i} \alpha_i^{(j)} = 1 \text{ and } \|\boldsymbol{\alpha}_i\|_0 \leq \kappa \leq N_i \end{aligned} \quad (4.1)$$

where  $\alpha_i^{(j)}$  is the  $j$ -th entry of  $\boldsymbol{\alpha}_i$  and  $\mathbf{V}_i$  is of full rank and defined in Equation (2.3).

If the columns in  $\mathbf{V}_i$  and  $\mathbf{y}$  are linearly independent, then the constraint  $\sum_{j=1}^{N_i} \alpha_i^{(j)} = 1$  ensures that the affine space spanned by  $\mathbf{V}_i \boldsymbol{\alpha}_i$  as  $\boldsymbol{\alpha}_i$  varies does not include the origin.

Since the  $\ell_0$ -norm of  $\boldsymbol{\alpha}_i$  is equal to the number of nonzero entries in  $\boldsymbol{\alpha}_i$ , the inequality  $\|\boldsymbol{\alpha}_i\|_0 \leq \kappa \leq N_i$  ensures that there are at most  $\kappa$  columns in  $\mathbf{V}_i$  which contribute to  $\mathbf{V}_i \boldsymbol{\alpha}_i$ . Since  $\boldsymbol{\alpha}_i$  has  $N_i$  entries, there are  $\binom{N_i}{\kappa}$   $\kappa$ -combinations of the valid columns (training samples) in  $\mathbf{V}_i$ . Note that as  $\binom{N_i}{\kappa}$  can be very large, we use a strategy described in Section 4.4, for reducing the number of  $\kappa$ -combinations of columns that are considered.

For the  $m$ -th training sample combination of the  $i$ -th class, we define the base matrix as follows.

$$\begin{aligned} \mathbf{W}_{i,m} &\doteq [\mathbf{w}_i^{(1)}, \dots, \mathbf{w}_i^{(\kappa)}] \\ \text{subject to } &\{\mathbf{w}_i^{(1)}, \dots, \mathbf{w}_i^{(\kappa)}\} \subseteq \{\mathbf{v}_i^{(1)}, \dots, \mathbf{v}_i^{(N_i)}\}. \end{aligned} \quad (4.2)$$

Using Equation (4.2), the subproblem of Equation (4.1) for the above mentioned  $\kappa$ -combination can be rewritten as follows.

$$r_i^{(m)}(\mathbf{y}) = \underset{\boldsymbol{\beta} \in \mathbb{R}^\kappa}{\operatorname{argmin}} \|\mathbf{y} - \mathbf{W}_{i,m} \boldsymbol{\beta}\|_2 \text{ subject to } \sum_{j=1}^{\kappa} \beta^{(j)} = 1 \quad (4.3)$$

where  $\beta^{(j)}$  is the  $j$ -th entry of  $\boldsymbol{\beta}$ .

Note that there are very mature algorithms for Equation (4.3). Interested readers are referred to [11, 12] for more details.

Using Equation (4.3), the solution of Equation (4.1) is obtained from the  $\binom{N_i}{\kappa}$  sub-solutions in that the distance  $r_i(\mathbf{y})$  is defined by

$$r_i(\mathbf{y}) = \min_m r_i^{(m)}(\mathbf{y}). \quad (4.4)$$

4.2. **NCSC.** Based on Equation (4.1), our proposed *Nearest Constrained Subspace Classifier* (NCSC) is summarized as Algorithm 1.

---

**Algorithm 1:** Nearest Constrained Subspace Classifier

---

**Input** : A query sample  $\mathbf{y}$ , training vectors partitioned to  $K$  classes and parameter  $\kappa$ .

**Output:** Class ID of  $\mathbf{y}$ .

```

for  $i \leftarrow 1$  to  $K$  do
  for  $m \leftarrow 1$  to  $\binom{N_i}{\kappa}$  do
    Obtain  $\mathbf{W}_{i,m}$  as in Equation (4.2);
    Calculate  $r_i^{(m)}(\mathbf{y})$  as in Equation (4.3);
  end
  Calculate  $r_i(\mathbf{y})$  as in Equation (4.4);
end
return  $\text{class}(\mathbf{y}) \leftarrow \text{argmin}_i r_i(\mathbf{y});$ 

```

---

Note, when  $\kappa = 1$ , Equation (4.1) becomes Equation (2.1) and when  $\kappa = 2$ , Equation (4.1) becomes Equation (2.2). This shows that NN and NFL are just two special cases of NCSC. Furthermore, we observe that the training sets used in NN are zero-dimensional affine subspaces, and the sets of feature lines used in NFL are one-dimensional affine subspaces.

If  $\kappa = 3$ , the NCSC becomes the NFP (Nearest Feature Plane) method. More mathematically, for the NFP method, when  $N_i \geq 3$ , Equation (4.1) can also be rewritten as follows.

$$r_i(\mathbf{y}) = \min_{\lambda_1, \lambda_2 \in \mathbb{R}} \left\| \mathbf{y} - \lambda_1 \mathbf{v}_i^{(a)} - \lambda_2 \mathbf{v}_i^{(b)} - (1 - \lambda_1 - \lambda_2) \mathbf{v}_i^{(c)} \right\|_2$$

subject to  $\{a, b, c\} \subseteq \{1, \dots, N_i\}$ . (4.5)

In Equation (4.5), when  $\lambda_1 > 0$ ,  $\lambda_2 > 0$  and  $1 - \lambda_1 - \lambda_2 > 0$ , the corresponding points are inside the triangle determined by  $\mathbf{v}_i^{(a)}$ ,  $\mathbf{v}_i^{(b)}$  and  $\mathbf{v}_i^{(c)}$ , otherwise the subspace points are outside the triangle or on its edges.

In Algorithm 1, the dimension of the affine subspaces is  $\kappa - 1$ . For convenience, we denote  $D_m, D_c, D_s, D$ , respectively as the dimensions of the data manifold, the affine subspace, the subspace used in NS and the feature space.

The value of  $D_c$  is

$$D_c = \kappa - 1 \geq 0. \tag{4.6}$$

In NN,  $D_c = 0$  and in NFL,  $D_c = 1$ . In NS, there is no constraint on the  $D_s$ , then, given  $N_i$  linearly independent training samples of a class, the dimension of subspace is the largest, namely,

$$D_s = N_i. \tag{4.7}$$

**4.3. Union of Affine Hulls and Data Manifold Approximation.** Given  $K$  classes, there are  $K$  constrained subspaces in NCSC. Each constrained subspace is a union of affine hulls. Here we give the explanation as follows. The  $i$ -th constrained subspace  $\mathbb{S}_i^{\text{NCSC}}$  is written as follows.

$$\mathbb{S}_i^{\text{NCSC}} = \{\mathbf{V}_i \boldsymbol{\alpha} \mid \boldsymbol{\alpha} \in \mathbb{R}^{N_i}, \|\boldsymbol{\alpha}\|_0 \leq \kappa \leq N_i \text{ and } \mathbf{1}^T \boldsymbol{\alpha} = 1\}. \quad (4.8)$$

Since the problem of Equation (4.1) can be divided into the  $\binom{N_i}{\kappa}$  subproblems of Equation (4.3), it is not difficult to show that  $\mathbb{S}_i^{\text{NCSC}}$  can be rewritten as a union of affine hulls. Namely

$$\begin{cases} \mathbb{S}_i^{\text{NCSC}} = \bigcup_{m=1}^{\binom{N_i}{\kappa}} \mathcal{H}_{i,m} \\ \mathcal{H}_{i,m} = \{\mathbf{W}_{i,m} \boldsymbol{\beta} \mid \boldsymbol{\beta} \in \mathbb{R}^{\kappa} \text{ and } \mathbf{1}^T \boldsymbol{\beta} = 1\} \end{cases} \quad (4.9)$$

where  $\mathcal{H}_{i,m}$  is the affine hull of the column vectors in  $\mathbf{W}_{i,m}$ .

Note that affine hull (i.e., affine subspace) is also referred to as linear manifold. This means that  $\mathbb{S}_i^{\text{NCSC}}$  can be viewed as an approximation to  $\mathcal{M}_i$  by using a series of linear manifolds.

Let  $\mathbb{S}_i^{\text{NS}}$  denote the linear subspace spanned by the  $N_i$  training samples of the  $i$ -th class.  $\mathbb{S}_i^{\text{NS}}$  is written as follows.

$$\mathbb{S}_i^{\text{NS}} = \{\mathbf{V}_i \boldsymbol{\alpha} \mid \boldsymbol{\alpha} \in \mathbb{R}^{N_i}\}. \quad (4.10)$$

From Equations (4.8) and (4.10), it is not difficult to find that  $\mathbb{S}_i^{\text{NCSC}}$  is a subset of  $\mathbb{S}_i^{\text{NS}}$  and in NCSC, the constrained subspaces defined as  $\kappa$  increases are nested. Namely

$$\mathbb{S}_i^{\text{NCSC}}|_{\kappa=1} \subset \mathbb{S}_i^{\text{NCSC}}|_{\kappa=2} \subset \cdots \subset \mathbb{S}_i^{\text{NCSC}}|_{\kappa=N_i} \subset \mathbb{S}_i^{\text{NS}}. \quad (4.11)$$

Note that  $\mathbb{S}_i^{\text{NCSC}}|_{\kappa=1}, \cdots, \mathbb{S}_i^{\text{NCSC}}|_{\kappa=N_i}$  and  $\mathbb{S}_i^{\text{NS}}$  can be regarded as some approximations to the data manifold  $\mathcal{M}_i$ . In this sense, we argue that NCSC/NS is an approximation to NMC (Nearest Manifold Classifier) and among  $\mathbb{S}_i^{\text{NCSC}}|_{\kappa=1}, \cdots, \mathbb{S}_i^{\text{NCSC}}|_{\kappa=N_i}, \mathbb{S}_i^{\text{NS}}$ , only one is the best approximation to  $\mathcal{M}_i$ . The approximation degree can be measured by the classification accuracies of NCSC with a variety of  $\kappa$  (or equivalently  $D_c$ ) and NS.

In order to make  $\mathbb{S}_i^{\text{NCSC}}$  the best approximation to  $\mathcal{M}_i$ , we argue that the common dimension of the affine subspaces in  $\mathbb{S}_i^{\text{NCSC}}$  should be equal to the dimension of  $\mathcal{M}_i$ . Otherwise the effectiveness of the linear approximation to a nonlinear manifold can not be guaranteed. Namely, we have

$$D_c = D_m. \quad (4.12)$$

In many applications,  $D$  is far larger than  $D_s$ ,  $D_c$  and  $D_m$ , namely,

$$D_m = D_c < D_s = N_i \ll D. \quad (4.13)$$

Although there are lots of techniques of feature dimension reduction for improving the algorithm efficiency, we argue that if the feature dimension  $D$  is near to  $D_s$ , or equivalently,  $D$  is near to  $N_i$  (the  $N_i$  training samples of the  $i$ -th class are linearly independent), the effectiveness of NS can not be guaranteed because  $r_1(\mathbf{y}), \dots, r_K(\mathbf{y})$  are all near to 0.

Also of particular note in Equation (4.13) is that, for a guaranteed performance of NCSC (and other classifiers), there exists a lower bound on  $N_i$ , which is also crucial for estimating  $D_m$ . More specifically, the lower bound should not be less than  $D_m$ . Namely, we have

$$N_i > D_m, \quad \forall i = 1, \dots, K. \quad (4.14)$$

Otherwise, the training samples are insufficient to guarantee an accurate estimate of  $D_m$  and high classification accuracy.

**4.4. Computational Complexity and Fast NCSC.** Given  $N_i$  training samples in the  $i$ -th class, the problem of Equation (4.1) is decomposed to  $\binom{N_i}{\kappa}$  subproblems of Equation (4.3). If  $N_i$  is large and  $\kappa \simeq \frac{N_i}{2}$ , then  $\binom{N_i}{\kappa}$  can be huge. This makes the computational complexity of Algorithm 1 very high.

To reduce the computational complexity of Algorithm 1, one simple strategy is to reduce  $\binom{N_i}{\kappa}$  to a smaller number. To do this, we assume that the nearest  $(\kappa - 1)$  neighbors of a data point  $\mathbf{x}$  and the data point itself in the same class are sufficient to capture the local manifold dimension at  $\mathbf{x}$ . Note that the neighborhood strategy is also employed in [13, 14] to estimate the intrinsic dimension of a dataset under the same assumption. We define the base matrix, whose columns vectors are  $\mathbf{x}$  and its  $(\kappa - 1)$  neighbors in the same class, as follows.

$$\mathbf{V}(\mathbf{x}) \doteq [\mathbf{v}_1, \dots, \mathbf{v}_\kappa] \quad (4.15)$$

where  $\mathbf{x} \in \{\mathbf{v}_1, \dots, \mathbf{v}_\kappa\}$ .

We implement fast NCSC, i.e., the NCSC via  $\kappa$ -neighbor representation, called NCSC-II, using Algorithm 2.

---

**Algorithm 2:** NCSC-II — fast NCSC via  $\kappa$ -neighbor representation

---

**Input** : A query sample  $\mathbf{y}$ , training vectors  $\{\mathbf{x}_1, \dots, \mathbf{x}_N\}$  partitioned to  $K$  classes and parameter  $\kappa$ .

**Output:** Class ID of  $\mathbf{y}$ .

**for**  $k \leftarrow 1$  **to**  $N$  **do**

    Calculate  $\mathbf{V}(\mathbf{x}_k)$  as in Equation (4.15);

$r(\mathbf{y}, \mathbf{x}_k) \leftarrow \min_{\boldsymbol{\beta} \in \mathbb{R}^\kappa} \|\mathbf{y} - \mathbf{V}(\mathbf{x}_k)\boldsymbol{\beta}\|_2$  subject to  $\mathbf{1}^T \boldsymbol{\beta} = 1$ ;

**end**

$m \leftarrow \operatorname{argmin}_k r(\mathbf{y}, \mathbf{x}_k)$

**return**  $\operatorname{class}(\mathbf{y}) \leftarrow \operatorname{class}(\mathbf{x}_m)$ ;

---



Given parameter  $\kappa$  and training samples  $\mathbf{x}_i^{(1)}, \dots, \mathbf{x}_i^{(N_i)}$  of the  $i$ -th class,  $\mathbb{S}_i^{\text{NCSC}}$  is formulated as the union of  $\binom{N_i}{\kappa}$  affine hulls. Since the complexity of Algorithm 1 depends on the  $\kappa$ -combinations of training samples, Algorithm 1 is NP-hard. In NCSC-II, most of the affine hulls are removed and the remaining ones define  $\mathbb{S}_i^{\text{NCSC-II}}$ , based on Equation (4.15) as follows.

$$\begin{cases} \mathbb{S}_i^{\text{NCSC-II}} = \bigcup_{m=1}^{N_i} \mathcal{H}_{i,m} \\ \mathcal{H}_{i,m} = \left\{ \mathbf{V}(\mathbf{x}_i^{(m)})\boldsymbol{\beta} \mid \boldsymbol{\beta} \in \mathbb{R}^\kappa \text{ and } \mathbf{1}^\top \boldsymbol{\beta} = 1 \right\} \end{cases} \quad (4.16)$$

By using the neighborhood representation, the computational complexity of Algorithm 2 is reduced to  $O(N)$ . We note that the properties/definitions of (4.6), (4.11), (4.12), (4.13) and (4.14) in NCSC still hold in NCSC-II.

**4.5. Intrinsic Dimension Estimation.** We argue that NCSC or NCSC-II with the fine-tuned parameter is expected to be the closest in performance to NMC (Nearest Manifold Classifier), which is believed to have the optimal classification accuracy. Furthermore, we contend that the classification accuracy of NCSC/NCSC-II is a function of  $D_c$ . We denote the function as  $f(D_c)$ .

We now have a scheme for estimating  $D_m$  of a labeled dataset.  $D_m$  is given on the assumption as follows.

$$D_m = \underset{D_c}{\operatorname{argmax}} f(D_c). \quad (4.17)$$

Equation (4.17) gives rise to two observations. First, given a labeled dataset,  $D_m$  is estimated by NCSC/NCSC-II. The second is that when  $D_m$  is learned, we have a tuned NCSC/NCSC-II, which outperforms many of its rivals such as NN, NFL, NS.

Note the NCSC/NCSC-II only has one parameter  $D_c$  (or equivalently,  $\kappa$ ). This assumes that all the classes have the same (local) intrinsic dimension. We call a dataset homogeneous, if the data classes are of the same (local) dimension, and a dataset inhomogeneous, if the data classes are of different dimension. For an inhomogeneous dataset, query samples can be classified by NCSC/NCSC-II if  $D_c$  is equal to the average (rounded) intrinsic dimension.

## 5. EXPERIMENTAL RESULTS

In this section, we apply the NCSC/NCSC-II to several publicly available image datasets. Note that the feature extraction usually serves as an important step for image classification. Effective features are beneficial to improve the classification accuracy. But it is not the focus of this study, thus, we keep the feature extraction simple.

In the following experiments, for feature extraction, we subtract the mean from each vectorized image and normalize the feature vectors to have a unit  $\ell_2$ -norm. Vectorization is carried out by concatenating the columns of each image.

### 5.1. Evaluation of NCSC as Dimension Estimator.

5.1.1. *PICS Dataset.* First, we present the results on the PICS/PES dataset [15]. The PICS/PES dataset is relatively small and contains 84 cropped facial images belonging to 12 subjects (7 images/subject  $\times$  12 subjects) with fixed eye location and different expressions. The image size is  $241 \times 181$  pixels.

Figure 2 shows the images of two subjects.

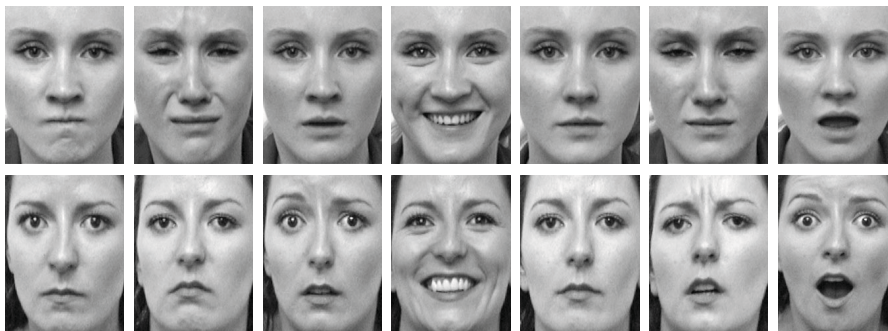


FIGURE 2. Image examples of the PICS/PES dataset. First row: images of one subject. Second row: images of another subject.

In order to get the classification accuracy from sufficient tests, the experiment contains multiple rounds of classifications. In each round of classification, we randomly select one image from each subject as the query samples (i.e., 1 image/subject  $\times$  12 subjects). The remaining 6 images of the same subject are chosen as the training samples (i.e., 6 images/subject  $\times$  12 subjects).

Figure 3 gives the classification rates of NCSC on the PICS/PES data with varying intrinsic dimension. Each classification accuracy in Figure 3 is obtained as the classification accuracy of 2016 query samples in 168 rounds (12 query images/round  $\times$  168 rounds).

After one round is complete, we randomly select the query and training samples for another round of classifications. After 168 rounds, the classification accuracy is calculated. The classification accuracy is given as follows.

$$f(D_c) = \frac{w}{W} \quad (5.1)$$

where  $w$  is the number of the correctly classified query samples and  $W$  is the total number of query samples. In this experiment,  $W = 2016$ .

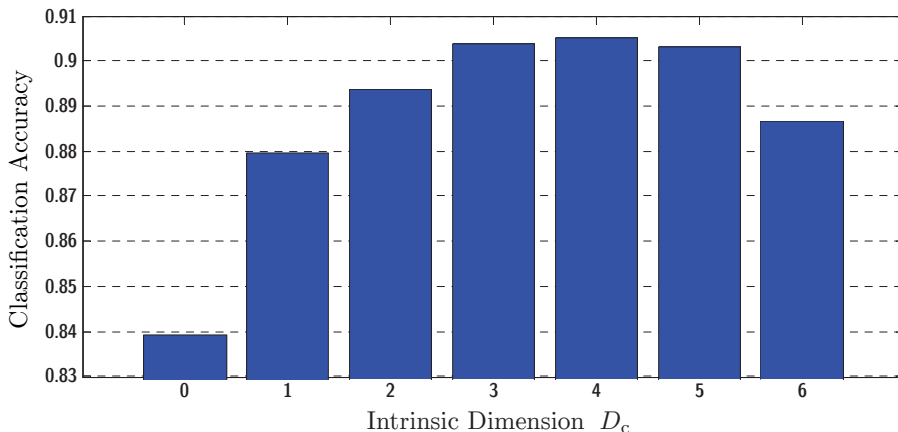


FIGURE 3. Classification accuracy of NCSC on the PICS/PES dataset over varying  $D_c$ .

Note that since the largest parameter  $\kappa$  of NCSC on the 72 training samples (6 training images/subject  $\times$  12 subjects) is 6 and  $D_c = \kappa - 1$ , the largest value of  $D_c$  is 5. In order to make a comprehensive comparison in Figure 3, we also give the classification accuracy of NS. When  $D_c = 6$ , it actually means the result of NS with  $D_s = 6$ .

In order to avoid unnecessary perturbations in the accuracies, the same random selections of training and query sets are preserved and repeated for different  $D_c$ . It is clear that none of NN ( $D_c = 0$ ), NFL ( $D_c = 1$ ) and NS ( $D_c = 6$ ) achieves the optimal classification.

According to the highest classification accuracies in Figure 3, our estimate of the intrinsic dimension of the PICS/PES dataset is  $D_m = 4$ .

5.1.2. *ORL Dataset.* Second, we give the experimental results on the ORL face dataset [16]. The dataset contains 400 images (10 images/subject  $\times$  40 subjects). The image size is  $112 \times 92$  pixels. The dimension of the data manifold of each subject is believed to be larger than one since the images were taken at different times, with variations in the lighting, facial expressions, facial details and poses.

Figure 4 shows the image examples of one subject from the ORL dataset.

Since the ORL dataset (400 images) is larger than the PICS/PES dataset (84 images), in order to avoid to the computational complexity problem of NCSC, we use NCSC-II for this experiment.

In order to be able to estimate  $D_m$ , we set  $N_i = 9$  for each class. In this setting, in one round of classifications, we have 360 training images (i.e., 9 training images/subject  $\times$  40 subjects) and 40 query images (i.e., 1 query image/subject  $\times$  40 subjects). After one round is completed, we randomly select the query and training samples for another round.



FIGURE 4. Image examples of a subject, with varying imaging conditions, such as illumination, facial expressions, details and orientations.

The range of  $D_c = 0, \dots, 9$  is traversed. Note that when  $D_c = 9$ , the result is actually the accuracy of NS with  $D_s = 9$ .

Figure 5 shows the classification accuracies of NCSC-II for the different  $D_c$ . Each accuracy is obtained as the result of 8000 query samples from 200 classification rounds (i.e., 40 query samples/round  $\times$  200 rounds). The classification accuracy is given by Equation (5.1) with  $W = 8000$ .

As in the first classification experiment, the random selections of training and query sets are preserved and repeated for classifications using different  $D_c$ .

Figure 5 shows that the highest classification accuracy appears at  $D_c = 6$ .

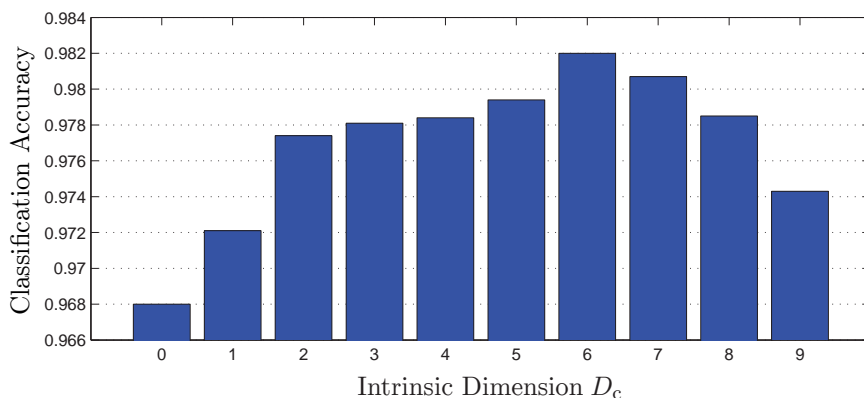


FIGURE 5. Classification accuracy on the ORL dataset for varying  $D_c$ .

5.1.3. *Comparison with Other Intrinsic Dimension Estimators.* Some well-known dimension estimators include MLE (Maximum Likelihood Estimation) [13], Correlation Dimension (hereafter referred to as Corr.Dim in this paper) [17, 18], PCA [19, 20] and their recent variations [21, 22, 14], etc. The statistical properties of these estimators, the best ways of evaluating them and the comprehensive comparisons of them are still open research areas.

In this part, we make a brief comparison between NCSC/NCSC-II and other estimators of PCA, MLE and Corr.Dim.

Among them, the PCA estimator, from its early proposal [19], to its later variants [20], is based on the classical principle component analysis, in which the estimate of dimension is determined by the number of eigenvalues not less than a predefined threshold.

The Corr.Dim estimator is summarized as follows. Given a dataset  $\{\mathbf{x}_1, \dots, \mathbf{x}_{N_i}\}$ , the following function is defined.

$$C(r) = \frac{2}{N_i(N_i - 1)} \sum_{i=1}^{N_i} \sum_{j=i+1}^{N_i} H(r - \|\mathbf{x}_i - \mathbf{x}_j\|_2) \quad (5.2)$$

where  $H(\cdot)$  is a unit step function satisfying if  $v > 0$ , then  $H(v) = 1$ , otherwise,  $H(v) = 0$ . The intrinsic dimension is estimated by plotting  $\log C(r)$  against  $\log r$  and calculating the slope of its linear part. Interested readers are referred to [17, 18] for more details.

The MLE estimator determines its estimate from  $\{\mathbf{x}_1, \dots, \mathbf{x}_{N_i}\}$  under the assumption that the closest  $k$  (where  $k$  is a fixed number and  $k > 2$ ) neighbors to a given point  $\mathbf{x}_i$  lie on the same manifold. The intrinsic dimension  $\hat{C}_m$  is estimated as follows.

$$\begin{cases} \hat{C}_k(\mathbf{x}_i) = \left[ \frac{1}{k-1} \sum_{j=1}^{k-1} \log \frac{T_k(\mathbf{x}_i)}{T_j(\mathbf{x}_i)} \right]^{-1} \\ \hat{C}_m = \frac{1}{N_i(k_2 - k_1 + 1)} \sum_{i=1}^{N_i} \sum_{k=k_1}^{k_2} \hat{C}_k(\mathbf{x}_i) \end{cases} \quad (5.3)$$

where  $T_k(\mathbf{x}_i)$  is the distance from  $\mathbf{x}_i$  to its  $k$ -th nearest neighbor. Interested readers are referred to [13] for more details.

Table ?? gives the intrinsic dimensions estimated by PCA, MLE, Corr.Dim and NCSC/NCSC-II. Note the tabulated estimates are given as the average over all classes. The PCA estimate is an integer for each class but its class average can be fractional while MLE and Corr.Dim only give fractional estimates for each class.

Since NCSC only gives integer estimates, for comparison purpose, we check the rounded estimates of PCA, MLE and Corr.Dim, namely 6 (PCA), 4 (MLE) and 6 (Corr.Dim) for the PICS dataset. For the ORL dataset, the rounded estimates are 9 (PCA), 4 (MLE) and 5 (Corr.Dim).

It has been widely accepted that the PCA estimator is not satisfactory for nonlinear manifolds, such as face image datasets. From Table ??, it is easy to see that the estimates of MLE and Corr.Dim are much closer to ours than those of PCA. For the PICS dataset, the rounded estimate of MLE ( $D_c = 4$ ) is equal to ours (by NCSC).

For the ORL dataset, the estimate of Corr.Dim ( $D_c = 5$ ) is closer to ours ( $D_c = 6$  by NCSC-II) than the estimate of MLE ( $D_c = 4$ ).

TABLE 1. Comparison of intrinsic dimension estimates by different estimators.

Dataset	Estimator			
	PCA	MLE	Corr.Dim	NCSC (proposed)
PICS	6	4.32	5.55	4 <sup>†</sup>
ORL	8.9250	4.34	5.09	6 <sup>‡</sup>

<sup>†</sup> Estimated by NCSC.

<sup>‡</sup> Estimated by NCSC-II.

**5.2. Evaluation of NCSC as Classifier.** If the intrinsic dimension of a given dataset is accurately estimated, NCSC/NCSC-II using the estimate can outperform many of its rivals.

In this experiment, we compare the classification performance of NCSC/NCSC-II with other related classifiers. The classifiers are evaluated by classifying the samples of the MNIST dataset. The MNIST dataset of handwritten digits contains 60000 training images and 10000 test images [23]. The digit images have been size-normalized and centered in a fixed-size image. The image size is  $28 \times 28$  pixels. Figure 6 shows some examples.



FIGURE 6. Examples of the MNIST dataset

Since the MNIST dataset is quite large, we use NCSC-II rather than NCSC to classify the query samples. In this experiment, we use the 10% MNIST samples for evaluation. More specifically, the training set contains the first 6000 images (600 images/class  $\times$  10 classes) and the query set contains the first 1000 images (100 images/class  $\times$  10 classes).

In the experiment, a variety of classifiers are used to classify the above mentioned 1000 query samples. The accuracies of the different classifiers are compared. Since the NCSC/NCSC-II framework depends on the intrinsic dimension  $D_c$ , we use the estimator of MLE or Corr.Dim to first estimate it.

Table ?? gives the dimensions estimated from the 10 training class (each contains 600 samples) by MLE and Corr.Dim. Since currently only the homogenous NCSC classifier is our interest, we have the rounded average estimate of 4 (over the 10 classes) by Corr. Dim and 8 (over the 10 classes) by MLE.

TABLE 2. Intrinsic dimension estimates by Corr.Dim and MLE.

Class Index	1	2	3	4	5	6	7	8	9	10
Corr.Dim*	3.16	2.58	4.24	3.78	4.08	4.43	3.47	3.54	3.94	3.43
MLE†	6.86	4.46	9.12	8.75	8.42	7.89	7.39	7.08	8.99	7.35

\* The rounded average estimate of Corr.Dim over the 10 classes is 4.

† The rounded average estimate of MLE over the 10 classes is 8.

To obtain the classification accuracies of related classifiers, we evaluate them on the uncorrupted query data and corrupted query data with the noise level  $\rho$  respectively equal to 10%, 20% and 30%.

The corrupted pixels are uniformly chosen in a target image. Since an MNIST image sample contains  $28 \times 28 = 784$  pixels, for the noise level  $\rho$ , the number of corrupted pixels is a rounded integer of  $784 \times \rho$ . The intensities of the corrupted pixels are uniformly distributed in  $\{i_{\min}, \dots, i_{\max}\}$ , where  $i_{\min}$  and  $i_{\max}$  are respectively the minimum and maximum intensity of the uncorrupted image. Figure 7 gives some MNIST samples and their corrupted versions.

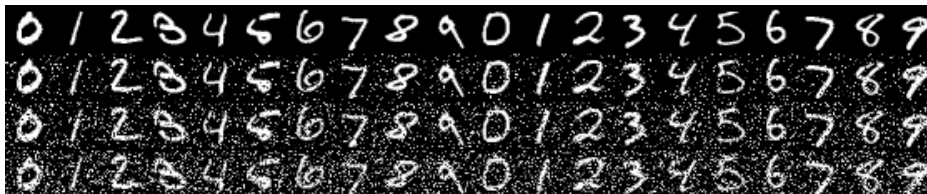


FIGURE 7. Some MNIST test samples and their corrupted versions with different noise levels. First row: uncorrupted samples. Second row: corrupted samples with noise level  $\rho = 10\%$ . Third row: corrupted samples with noise level  $\rho = 20\%$ . Bottom row: corrupted samples with noise level  $\rho = 30\%$ .

Table 3 gives the accuracies of NN, NFL, NS and NCSC-II with  $D_c$  respectively equal to 1, 4 and 8 for classifying the 1000 query samples (100 query samples/class  $\times$  10 classes) respectively corrupted by different noise levels.

Note each training class contains 600 samples, which in fact are too many for NFL to deal with. In order to obtain the distance of a query sample to a given class, NFL computes the projection distances of a query sample to  $\binom{600}{2} = 179700$  feature lines. The computational cost is very high. Thus, we could not obtain in an acceptable time the classification accuracy of NFL, which happens to be NCSC with  $D_c = 1$ . For

comparison purpose, we give the classification accuracy of NCSC-II with  $D_c = 1$ , which is the fast version of NFL.

We are particularly interested in the classification accuracies of NCSC-II using the  $D_c$  respectively estimated by Corr.Dim and MLE, i.e.,  $D_c = 4$  and  $D_c = 8$ . Table 3 shows the results using the estimates by Corr.Dim and MLE. It is easy to see that NCSC-II using the estimate by MLE yields better classification accuracies than those associated with Corr.Dim. It also shows that the highest accuracy (96.0%) is obtained by NCSC-II with the estimate by MLE ( $D_c = 8$ ) on the uncorrupted MNIST data samples.

From this point of view, we contend that *for the MNIST dataset, the estimate by MLE is better than the estimate by Corr.Dim.*

The NS algorithm fails in this experiment, yielding the classification accuracies not larger than 54.7%. As mentioned in previous sections, NS can be viewed as a high dimensional extreme of NCSC and NCSC-II. In this experiment on the MNIST dataset ( $600 \times 10$  training samples), the 10 subspaces (corresponding to the 10 training classes) employed by NS are intrinsically nearly 600 dimensional<sup>1</sup>. The intrinsic dimension is unnecessarily high and there is a high probability that the various subspaces have significant overlaps. See Expression (4.11) for more on this issue.

Furthermore, note, as another extreme, NN yields the second lowest accuracy in this experiment.

TABLE 3. Comparison of classification accuracies of several subspace-based classifiers.

Noise Level		0%	10%	20%	30%
NN		92.3%	91.6%	91.9%	91.6%
NFL #		—			
NCSC-II	$D_c = 1$ †	93.4%	93.0%	93.4%	92.1%
	$D_c = 4$ (Corr.Dim)	94.9%	94.1%	94.0%	91.9%
	$D_c = 8$ (MLE) *	96.0% ‡	94.6%	94.0%	92.1%
NS		54.7%	12.7%	12.5%	10.5%

# Unable to obtain experimental results in an acceptable time.

† Corresponding to the fast NFL classifier, i.e., NCSC-II with  $\kappa = 2$ .

\* Corresponding to the optimal classification performance, using  $D_c$  estimated by MLE.

‡ The highest classification accuracy in this experiment.

Table 3 supports to our claim that with appropriately estimated dimension parameter, NCSC (or NCSC-II as demonstrated in this experiment) as a parameterized classifier, can outperform its rivals. Its classification accuracy depends on the accuracy of the estimated dimension.

<sup>1</sup>The intrinsic dimension is equal to the rank of the matrix whose columns are the 600 training vectors of a target class.



**5.3. Comparison of Run Time.** Table 4 gives the comparison of the run time of classifying one query sample by a variety of classifiers, including NN, NFL NS and NCSC-II, respectively on the MNIST data with a small training set of 6000 images, (i.e., 600 images/class  $\times$  10 classes) and a large training set of 60000 images (i.e., the complete MNIST training set of 10 classes, each approximately having 6000 images).<sup>2</sup>

TABLE 4. Comparison of run time of different classifiers.

Traing Set Size	Run Time (second)					
	NN	NS	NFL	NCSC-II		
				$D_c = 1$	$D_c = 4$	$D_c = 8$
6000	0.05	1.53	> 35 minutes	7.03	8.47	8.64
60000	0.49	10.70	> 50 hours	70.70	83.51	88.32

The classifications on the large training set yield a similar classification accuracy comparison to that given in Table 3, where the classification accuracies of NN and NS are less than those of NCSC respectively with  $D_c = 1, 4$  and 8.<sup>3</sup>

The run time in Table 4 is given as the average time of 100 independent classifications.<sup>4</sup>

Among the evaluated classifiers, NFL is the most time-consuming. The time of classifying a query sample by NFL is larger than 35 minutes with the small training set and 50 hours with the large training set.

Using the small training set, NCSC (with  $D_c = 1, 4$  and 8) yields moderate run time between 7 – 9 seconds. Using the large training set, whose size is 10 times that of the small training set, NCSC-II yields the run time between 70 – 90 seconds.<sup>5</sup> It is shown that the time complexity of NCSC-II is proportional to the size of training set.

## 6. CONCLUSION

We propose a novel classifier, called NCSC, and a fast version NCSC-II. The proposed algorithms can be used as an intrinsic dimension estimator for a labeled dataset or a classifier when the dimension parameter is given.

The proposed NCSC/NCSC-II generalizes some classical classifiers including NN (Nearest Neighbor), NFL (Nearest Feature Line) and has a close relation to NS (Nearest Subspace). We proved that NN and NFL are two special cases of low-dimensional

<sup>2</sup> The environment for this experiment is MATLAB on an x64 PC with 32GB memory and an Intel CPU at 3.2 GHz.

<sup>3</sup> NS fails to accurately classify query samples, yielding a classification accuracy of approximate 55% for the small training set and approximate 23% for the large training set.

<sup>4</sup>In the run time experiments for NCSC-II, we assume that the neighborhood information of each training sample is obtained before classification.

<sup>5</sup> With the help of parallel computing, the run time can be significantly reduced for practical uses.

NCSC (with the dimension parameter  $D_c$  respectively equal to 0 and 1) while NS is closely associated with the highest dimensional NCSC.

The NCSC framework is a constrained linear regression problem under the least squares principle. First, the regression coefficients are regularized to ensure that the sum of all coefficients is equal to 1. Second, the regression coefficient vector is sparse under the assumption that the data manifold has a relatively low dimension.

We use  $\ell_0$ -norm to ensure the sparsity of the coefficient vector. Then, we define the constrained subspace dimension given the bound on the  $\ell_0$ -norm of coefficient vector. We contend that as an approximation to the target data manifold, the constrained subspaces should all have a dimension equal to the manifold dimension in order to approximate the manifold more accurately.

In order to reduce the computational complexity of NCSC, which depends heavily on the number of subsets of the training samples, we further propose a fast version of NCSC, called NCSC-II. Under the assumption that the nearest neighbors of a target data point of the same class can capture the local intrinsic dimension, NCSC-II employs a  $\kappa$ -neighbors representation to model the sparsity of coefficient vector. Using the  $\kappa$ -neighbors representation, the computational complexity is significantly reduced.

We evaluate NCSC/NCSC-II respectively as an estimator and a classifier on several publicly available datasets and compare the results of NCSC/NCSC-II with those obtained by the MLE, Corr.Dim estimators and the NN, NFL, NS classifiers.

Experiments show NCSC/NCSC-II can serve either as an estimator or a classifier with good performance. NCSC/NCSC-II can serve as a benchmark in terms of classification accuracy to evaluate the performances of other estimators. On the other hand, when an appropriate dimension parameter is given, NCSC/NCSC-II outperforms a wide range of its subspace-based rivals.

#### ACKNOWLEDGMENTS

This work was partly supported by the National Natural Science Foundation of China.

#### REFERENCES

- [1] G. E. Hinton, P. Dayan, and M. Revow, "Modeling the manifolds of images of handwritten digits," *IEEE Transactions on Neural Networks*, vol. 8, pp. 65–74, 1997.
- [2] M. Turk and A. Pentland, "Eigenfaces for recognition," *Journal of Cognitive Neuroscience*, vol. 3, no. 1, pp. 71–86, 1991.
- [3] D. Broomhead and M. Kirby, "The Whitney reduction network: A method for computing autoassociative graphs," *Neural Computation*, vol. 13, no. 11, pp. 2595–2616, 2001.
- [4] J. Tenenbaum, V. Silva, and J. Langford, "A global geometric framework for nonlinear dimensionality reduction," *Science*, vol. 290, no. 5500, pp. 2319–2323, 2000.

- [5] D. L. Donoho and C. Grimes, “Hessian eigenmaps: Locally linear embedding techniques for high-dimensional data,” *Proceedings of the National Academy of Sciences of the United States of America*, vol. 100, no. 10, p. 5591, 2003.
- [6] S. Roweis and L. Saul, “Nonlinear dimensionality reduction by locally linear embedding,” *Science*, vol. 290, no. 5500, pp. 2323–2326, 2000.
- [7] K. Weinberger and L. Saul, “Unsupervised learning of image manifolds by semidefinite programming,” in *Proceedings of the 2004 IEEE Computer Society Conference on Computer Vision and Pattern Recognition, 2004. CVPR 2004.*, vol. 2. IEEE, 2004, pp. II–988.
- [8] Z. Zhang and H. Zha, “Principal manifolds and nonlinear dimensionality reduction via tangent space alignment,” *Journal of Shanghai University (English Edition)*, vol. 8, no. 4, pp. 406–424, 2004.
- [9] M. Belkin and P. Niyogi, “Laplacian eigenmaps and spectral techniques for embedding and clustering,” in *Advances in Neural Information Processing Systems 14*. MIT Press, 2001, pp. 585–591.
- [10] S. Z. Li and J. Lu, “Face recognition using the nearest feature line method,” *IEEE Transactions on Neural Networks*, vol. 10, pp. 439–443, 1999.
- [11] T. Coleman and Y. Li, “A reflective newton method for minimizing a quadratic function subject to bounds on some of the variables,” *SIAM Journal on Optimization*, vol. 6, no. 4, pp. 1040–1058, 1996.
- [12] W. M. Gill P.E. and M. Wright, *Practical Optimization*. London, UK: Academic Press, 1981.
- [13] E. Levina and P. J. Bickel, “Maximum likelihood estimation of intrinsic dimension,” in *Advances in Neural Information Processing Systems 17*, L. K. Saul, Y. Weiss, and I. Bottou, Eds., Cambridge, MA, December 2005, pp. 777–784.
- [14] K. Carter, R. Raich, and A. Hero, “On local intrinsic dimension estimation and its applications,” *IEEE Transactions on Signal Processing*, vol. 58, no. 2, pp. 650–663, 2010.
- [15] Stirling, “Psychological image collection at Stirling (PICS),” [http://pics.psych.stir.ac.uk/2D\\_face\\_sets.htm](http://pics.psych.stir.ac.uk/2D_face_sets.htm).
- [16] AT&T, “The database of faces,” 2002, <http://www.cl.cam.ac.uk/research/dtg/attarchive/facedatabase.html>.
- [17] P. Grassberger and I. Procaccia, “Measuring the strangeness of strange attractors,” *Physica D: Nonlinear Phenomena*, vol. 9, no. 1, pp. 189–208, 1983.
- [18] F. Camastra and A. Vinciarelli, “Estimating the intrinsic dimension of data with a fractal-based method,” *IEEE Transactions on Pattern Analysis and Machine Intelligence*, vol. 24, no. 10, pp. 1404–1407, 2002.
- [19] K. Fukunaga and D. Olsen, “An algorithm for finding intrinsic dimensionality of data,” *IEEE Transactions on Computers*, vol. 100, no. 2, pp. 176–183, 1971.
- [20] J. Bruske and G. Sommer, “Intrinsic dimensionality estimation with optimally topology preserving maps,” *IEEE Transactions on Pattern Analysis and Machine Intelligence*, vol. 20, no. 5, pp. 572–575, 1998.
- [21] A. massoud Farahmand, C. Szepesvári, and J. Audibert, “Manifold-adaptive dimension estimation,” in *Proceedings of the 24th international conference on Machine learning*, 2007, pp. 265–272.
- [22] M. Fan, H. Qiao, and B. Zhang, “Intrinsic dimension estimation of manifolds by incising balls,” *Pattern Recognition*, vol. 42, no. 5, pp. 780–787, 2009.
- [23] Y. LeCun and C. Cortes, “The MNIST database of handwritten digits,” <http://yann.lecun.com/exdb/mnist/>.